Nanoscale Advances

ROYAL SOCIETY OF CHEMISTRY

PAPER

View Article Online
View Journal | View Issue



Cite this: *Nanoscale Adv.*, 2024, **6**, 5663

# A highly reactive soybean oil-based superhydrophobic polyurethane film with long-lasting antifouling and abrasion resistance†

Junming Huang,[ab] Genzheng Sha,[bc] Minghui Cui,[bc] Mengqiu Quan,[bc] Yuqing Wang,[bc] Yao Lu,*[a] Jin Zhu[bc] and Jing Chen *[bc]

Received 16th August 2024
Accepted 8th September 2024

DOI: 10.1039/d4na00674g

rsc.li/nanoscale-advances

Superhydrophobic polyurethanes offer robust hydrophobicity and corrosion resistance. However, it is essential to consider the durability and environmental constraints associated with these materials. This study prepared a bio-based superhydrophobic polyurethane coating film using epoxidized soybean oil, superhydrophobically modified silica nanoparticles, and OH–PDMS–OH as surface modifiers. The coating film exhibited sustained super-hydrophobicity and an excellent antifouling effect for pu-erh tea and edible oils, among other substances, after 14 days of immersion in solutions with different pH values, 28 days of exposure to air, and 2000 abrasion cycles. This finding can be applied to the development of daily indoor and outdoor antifouling protective coatings and provides a new method for the preparation of green and durable superhydrophobic antifouling coating films.

## 1. Introduction

Polyurethane, as one of the most widely used and highly researched protective products in the world today, is extensively applied in various products in our daily lives. These include coatings for leather,[1] high-strength adhesives for concrete,[2] artificial blood vessels,[3] controlled drug release[4] and more.

Haibo Wang *et al.* reported a PPG-based corrosion-resistant and hydrophobic self-healing polyurethane coating with mesoporous silica loaded with $CeO_2$ and Phen, and the coating has a maximum WCA = 108°.[5] This type of polyurethane, which consists of petroleum-based polyols and isocyanates, is easier to synthesize but is usually only incinerated or landfilled after use, resulting in soil and ecosystem contamination.[6] In light of the increasing depletion of petroleum resources and global climate warming, this type of polyurethane does not align with the concept of green and sustainable development.[7] To address such issues, substituting petroleum-based polyols with bio-based polyols for synthesizing polyurethane has gained widespread favor among researchers.[8] In a study by Zhou *et al.*, they utilized castor oil and long-chain hydrophobic chain extenders to create water-resistant polyurethane with strong hydrophobic properties and a corrosion-resistant water contact angle (WCA) of 87.5°.[9] Vegetable oil, as one of the most common bio-based sources, is characterized by its low toxicity, biodegradability, and long alkyl chains that enhance the hydrophobic properties of materials. Although the low molecular weight of vegetable oil can ultimately affect the tensile strength and glass transition temperature of polyurethane, thus limiting its applications, the hydroxyl groups, triglycerides, and carbon–carbon double bonds in its structure provide different reactive sites. Therefore, vegetable oil-based polyurethanes have great potential for functionalization.[10]

The lotus leaf effect in nature, butterfly wings and insect epidermis have inspired researchers to study superhydrophobic surfaces.[11] Superhydrophobic surfaces have a very high contact angle (CA ≥ 150°). Several superhydrophobic polyurethane materials (films,[12] sponges[13] and coatings[14]) have been studied in recent years. The current research on superhydrophobic coatings is primarily focused on applications such as acid and alkali resistant and corrosion protection coatings,[15,16] highly efficient separators of oil–water emulsion,[17,18] mechanically robust and anti-icing application coatings,[19,20] self-healing superhydrophobic specialty coatings,[21] and UV-resistant, self-cleaning coatings.[22] Fluorine atoms possess strong hydrophobic and oleophobic properties; the traditional method for preparing superhydrophobic polyurethane involves using fluorides chemically bonded to the polyurethane structure, or embedding or spraying fluoride-modified nanoparticles onto the polyurethane.[23,24] Despite the advantages of fluorinated reagents, their potentially long-lasting effects on the environment, the accumulation of fluoride, which can pose a health hazard (endocrine, fertility), and the relatively high cost of

[a]*Department of Materials Science and Engineering, Shenyang University of Chemical Technology, Shenyang 110142, PR China. E-mail: luyao915@syuct.edu.cn*

[b]*Key Laboratory of Bio-based Polymeric Materials Technology and Application of Zhejiang Province, Laboratory of Polymers and Composites, Ningbo Institute of Material Technology and Engineering, Chinese Academy of Sciences, Zhejiang, Ningbo 315201, PR China. E-mail: chenjing@nimte.ac.cn*

[c]*University of Chinese Academy of Sciences, Beijing, 100039, PR China*

† Electronic supplementary information (ESI) available. See DOI: https://doi.org/10.1039/d4na00674g

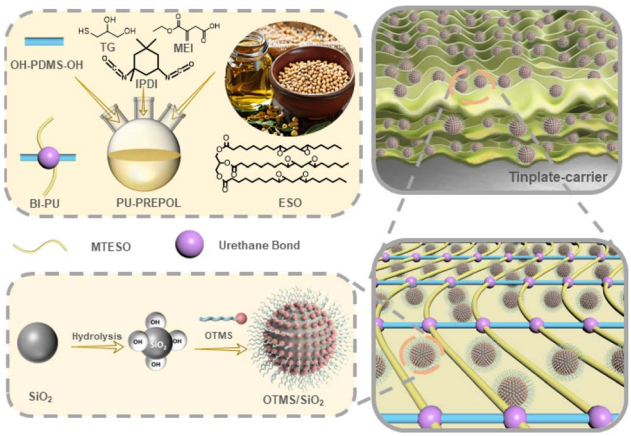


Fig. 1 The preparation process of the composite coating films.

fluorinated reagents have greatly limited their use in everyday applications.[25]

During the curing of polyurethane, the Si–O–Si chains in PDMS migrate from the interior of the molecular segments to the surface of the coating driven by low surface energy,[26,27] so that PDMS has the same hydrophobic properties as fluorinated reagents and is considered to be an alternative to fluorinated reagents due to their inherent good biocompatibility, the low burden on the environment during production and relatively low costs.[28] In recent years, in the field of hydrophobicity, researchers have chemically bonded PDMS with different end groups onto polyurethane substrates to produce a protective coating film with excellent hydrophobicity, oleophobic, and anti-icing properties.[29–31]

In this study, a high hydroxyl value polyol (with a hydroxyl value of 1.89 mm $g^{-1}$) with multiple reaction sites was prepared from renewable epoxidized soybean oil (ESO), mono-ethyl itaconic acid (MEI), and monothioglycerol. A biobased superhydrophobic material was produced by combining octadecylsilane-modified fumed silica nanoparticles and mono-terminal dihydroxy PDMS, which serve as a low-surface-energy modifier and a biobased superhydrophobic composite material, respectively. The coating film was subjected to comprehensive evaluation to ascertain its resilience to superhydrophobicity under diverse application scenarios, including abrasion, acid and alkali corrosion, and outdoor exposure. Additionally, its antifouling and self-cleaning properties were assessed under varying life use conditions, such as methylene blue solution, methyl orange solution, pu-erh tea, edible oil, and more. The film is anticipated to serve as a protective coating on a range of materials, both indoors and outdoors. The synthesis process is illustrated in Fig. 1.

# 2. Experimental

## 2.1 Materials

Epoxy soybean oil, mono-ethyl itaconic acid, monothioglycerol, 2-hydroxy-2-methylpropiophenone (1173), hydroquinone, triphenylphosphine, cyclohexanol, 2-chloro-1,3,2-dioxaphospholane, and nano-silicon dioxide, were bought from Shanghai Aladdin Biochemical Technology Co., Ltd, China. Sylgard 184 (OH–PDMS–OH) was obtained from Dow Corning. Sodium bicarbonate, dichloromethane, acetone, and ethyl acetone were all purchased from Sinopharm Chemical Reagent Co., Ltd, China.

## 2.2 Preparation of epoxy soybean oil-based polyols

The free radical polymerization of 15.815 g (0.1 mol) of mono-ethyl itaconic acid, 26.56 ml of epoxidized soybean oil (0.1 mol of the epoxy group), 0.424 g (1 wt%) of triphenylphosphine as the catalyst, and 0.085 g (0.2 wt%) of hydroquinone were placed in a 250 ml three-necked round-bottomed flask with a magnetic stirrer and thermometer and reflux condenser. First, they were stirred at 800 rpm at 80 °C for 30 min, then heated to 125 °C, and kept at 120 °C for 3.5 h. To eliminate the influence of unreacted mono-ethyl itaconic acid on the subsequent reaction, the modified product was purified. The product was dissolved in dichloromethane and it was allowed to stand and wash multiple times through a separating funnel with 1 wt% $NaHCO_3$ aqueous solution and a large amount of deionized water. Then MESO was obtained after removing the solvent using a rotary evaporator.[32] The synthesis route is shown in Fig. 2a.

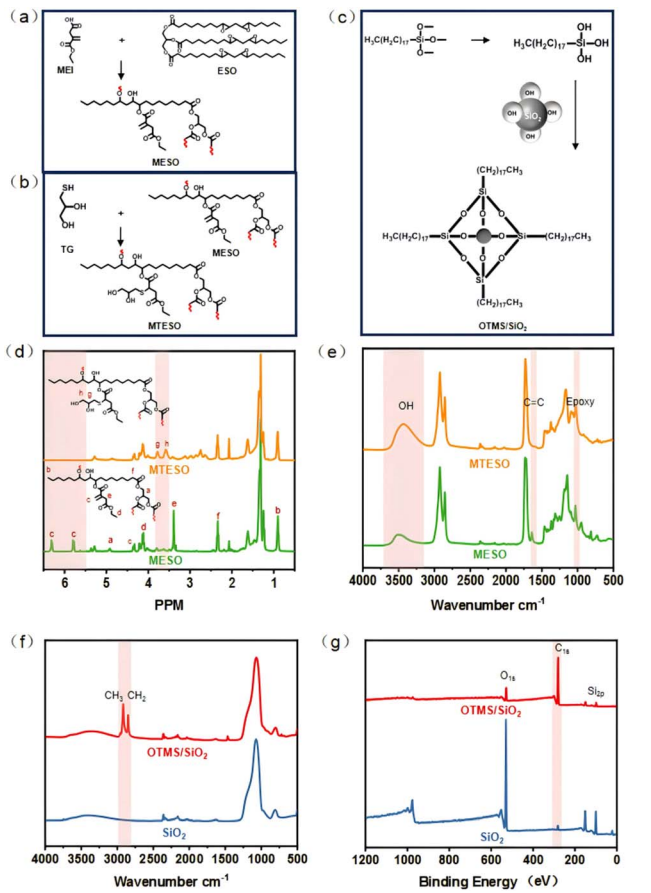


Fig. 2 Reaction process of MESO (a), reaction process of MTESO (b), reaction process of superhydrophobic silica (c), $^1$H NMR spectra of polyol (d), FTIR spectra of polyol (e), FTIR spectra of superhydrophobic silica (f), and XPS analysis of super-hydrophobic silica (g).

Step two: enhancing the hydroxyl value of polyols through the thiol ene click reaction. 10.816 g (0.1 mol) monothioglycerol, 0.532 g (1 wt%) 1173, 50 ml acetone and the product of step one were placed in a 250 ml volumetric flask and reacted for 5 hours at 800 rpm speed and under UV light irradiation. At last, the product was dissolved in ethyl acetate, an excess of saturated NaCl solution was added, and the product was extracted on four occasions and then vaporized to obtain MTESO. The synthesis route is shown in Fig. 2b.

### 2.3 Preparation of superhydrophobic bio-based polyurethane

First, super-hydrophobically modified nano-silica was synthesized. 1 g OTMS was sonicated in 10.0 g of ethanol : water (90 : 10) for 10 min and acetic acid was added into the solution mixture to adjust the pH to 3–4. Then 0.5 g of silica was added and the solution system was stirred for 180 min. Finally, OTMS/$SiO_2$ was obtained by repeated centrifugation and washing. The synthesis route is shown in Fig. 2c.

To obtain a superhydrophobic coating film solution, polyols were dissolved in DMF and a certain amount of superhydrophobic silica particles and OH–PDMS–OH were mixed with IPDI and DBTDL. The synthesis formula is shown in Table S1.† Sample names are indicated by abbreviations such as 10% P/PU represents PDMS added at 10% wt. of polyol. 10% O/Si–20% P/PU represents OTMS-modified $SiO_2$ added at 10% wt. of 20% polyols and IPDI. Preparation of polyurethane by the prepolymerization method: the prepolymer solution is reacted at 80 °C for 5 minutes and then poured into a PTFE plate. It was cured at 60 °C for 8 hours.

### 2.4 Characterization

**FT-IR.** Fourier transform infrared (FT-IR) spectroscopy was performed using a microinfrared spectrometer (Cary660 + 620, Agilent, USA) to obtain FT-IR data (500–4000 $cm^{-1}$).

**Transmittance.** The transmittance of the coating film was measured using an ultraviolet-visible near-infrared spectrophotometer (PerkinElmer, America) in a region from 300 to 800 nm. The wavelength indicating transparency of the coating film is 500 nm.

**$^1$H NMR spectra.** $^1$H NMR was examined using a 400 MHz AVANCE III Bruker NMR spectrometer (Bruker, Switzerland) and acetone-d6 as solvent.

**Thermogravimetric analysis (TGA).** Before testing, all samples were dried at 60 °C for 8 h, then heated from room temperature to 800 °C at a heating rate of 20 °C $min^{-1}$ in an inert environment ($N_2$) using a thermogravimetric analyzer (Mettler Toledo, China), and the thermal stability of materials was evaluated.

**Testing of mechanical properties.** Tensile tests were performed on an LPC (Z1.0, Zwick, Germany), and tensile performance testing on PU samples at room temperature was performed using an electronic universal testing machine.

**Contact angle measurement.** In these experiments, a contact angle meter (OCA25, Data Physics Instruments, Germany) was used to measure 2 μl water droplets used as the standard to test the surface wettability of the sample and to evaluate the persistence of superhydrophobic surfaces in different environments.

The superhydrophobic sample was placed face down on a 2000 SiC sandpaper with a load weight of 100 g. Then, the sample was horizontally pulled at a constant speed for 10 centimeters and the contact angle was measured after 500, 1000, 1500, and 2000 cycles, respectively.

In the deionized water as the control group, solutions with different pH values were set up and the samples were completely immersed in them. Two weeks later, the sample was removed and contact angle testing was performed. The superhydrophobic samples were exposed to the sun and rain for different periods and then tested for the contact angle.

**Surface morphology.** The surface morphologies of PU were observed using a thermal field emission scanning electron microscope (SEM, Verios G4 UC, Thermo Scientific), through this analysis method it is known the reason why the material can in-creased hydrophobicity. Before testing, all samples were dried at 60 °C for 8 h and then sputter-coated with approximately 10 nm of platinum using an anion sputter coater (E-1045, Hitachi).

**Pollution resistance test.** The sample was vertically immersed into methylene blue solution, methyl orange solution, tea, edible oil, and other liquids to study the anti-fouling ability of the coating film.

**Determination of hydroxyl value of polyols.** Method of referencing literature.[33] The hydroxyl values of the synthesized polyols (MTESO) were determined using a nuclear magnetic resonance spectrometer. First, 10 mg of polyols was placed into a centrifuge tube and 500 μl V deuterated chloroform : V pyridine = 1 : 1.6 was added. Then 100 μl acetylacetone chromium solution was added which was used as a buffer reagent (5 mg $ml^{-1}$ dissolved in the above-mixed solvent) and 10 mg cyclohexanol was added as the internal standard. Shake and dissolve thoroughly, then added 70 μl TMDP.

## 3. Results and discussion

### 3.1 Material synthesis and characterization

Acetone-d6 was chosen as the solvent. Fig. 2d shows the $^1$H NMR spectra of epoxy soybean oil-based polyols and soybean oil. The peaks at 6.32 and 5.82 ppm belong to the protons c on the carbon–carbon double bond structure from mono-ethyl itaconic acid,[34] and peaks at 3.42 and 4.1 ppm come from the protons e and d on the mono-ethyl itaconic acid. The peaks at 3.62 and 3.85 ppm come from the protons g and h of monothioglycerol. The peaks at 4.85, 0.89, and 2.38 ppm belong to the protons a, b, and f of the soybean oil structure. The integrated area of the peak belongs to proton c on the 6.32 ppm carbon–carbon double bond and the integral area of the peak at 0.89 ppm corresponds to the protons b on terminal $-CH_3$ of soybean oil. The grafting rate of itaconic acid mono-ethyl ester can be determined using the equation $G_{C=C} = 9 \times I_{\text{double bond}}/I_{CH_3}$, $G_{C=C} = 2.65$. It can be inferred from this that an average of 2.5 mono-ethyl itaconic acid is integrated into the structure of epoxy soybean oil.

FTIR can determine the occurrence and termination of the reaction. Fig. 2e shows the FTIR spectra of poxy soybean oil-based polyols and soybean oil. The success and completion of ring opening and click reactions can be demonstrated by the peak of carbon–carbon double bonds that first appears and then disappears at around 1640 $cm^{-1}$. The disappearance of the peak of the epoxy group at approximately 827 $cm^{-1}$ indicates the success of the impurity removal step. And the increase in the hydroxyl value of polyols can be estimated by the change in peak at 3300–3500 $cm^{-1}$. Fig. 2f shows the FTIR spectra of fumed nano-$SiO_2$ and superhydrophobically modified $SiO_2$. At 2840 $cm^{-1}$ and 2920 $cm^{-1}$, corresponding to the stretching vibrations of $CH_3$ and $CH_2$, the absorption bands are attributed to the long alkyl chains brought by OTMS. However, the self-condensation of OTMS may occur during the hydrolysis process, making it difficult to rule out the possibility that $CH_2$ may also come from self-condensation. Fig. 2g shows the XPS of OTMS modified the $SiO_2$. It is evident that $SiO_2$ is composed of the elements Si and O. Superhydrophobically modified $SiO_2$ comprises the elements Si, O, and C. The presence of up to 81.14% carbon in superhydrophobically modified silica confirms the successful integration of the hydrophobic modifier OTMS into the silica.

### 3.2 Effect of OH–PDMS–OH and OTMS/$SiO_2$ loading on coating film physical properties

OH–PDMS–OH and silica are used together as hydrophobic modifiers. Therefore, it is necessary to consider the influence of different loading amounts on the physical properties of the coating film. It was heated from room temperature to 800 °C at a heating rate of 20 °C $min^{-1}$ under an inert environment ($N_2$) using a thermogravimetric analyzer. Fig. 3a and b show the TGA-DTG results. It can be seen that the thermal decomposition process of polyurethane mainly consists of two stages. It is located around 250 °C and 380 °C respectively. The initial stage, spanning a temperature range of 20 °C to 250 °C, is characterized by a loss in weight due to the breakage of residual small molecules and fatty acid chains. This phenomenon is attributed to the evaporation of physically adsorbed water and the breaking of small molecule fatty acid chains during synthesis. The second stage, spanning 250 °C to 380 °C, exhibits the most rapid rate of thermal decomposition. This stage encompasses the degradation of carbon and sulfur single bonds and urethane carbamate bonds within the hard segments of the urethanes.[33] The temperature range from 380 °C to 500 °C is primarily associated with the degradation of the soybean oil-based soft segments of the urethanes and the siloxane chains of OH–PDMS–OH. As illustrated in Fig. 3a and b the thermal decomposition rate of polyurethane exhibits a decline with the incorporation of both OH–PDMS–OH and superhydrophobically modified $SiO_2$ into the system. This phenomenon can be attributed to the chemical bonding of the OH–PDMS–OH moiety added between the chains of polyurethane macromolecules, which results in the formation of a cross-linked network structure. This process markedly enhances intermolecular interactions. Furthermore, flame-retardant silicone serves to impede the transfer of heat.[35]

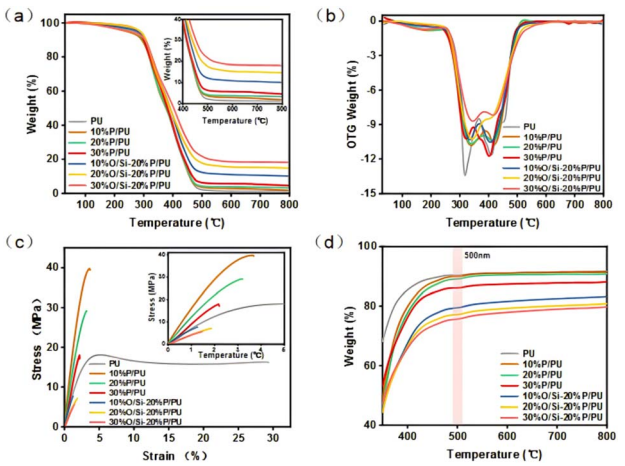


Fig. 3 The TG results of PU (a), the DTG results of PU (b), the stress–strain curve of PU (c), and the visible light transmission degree of PU (d).

Fig. 3c shows the mechanical properties of cured samples by tensile testing. The tensile strength of the polyurethane without the modifier was 18 MPa and the elongation at break was 29%. The incorporation of OH–PDMS–OH resulted in an enhancement of the tensile strength of PU up to 40 MPa. However, both the tensile strength and elongation at break of PU exhibited a decline with the increase in the addition amount. Furthermore, the incorporation of superhydrophobically modified silica resulted in a further reduction in both the tensile strength and elongation at break of PU. The incorporation of OH–PDMS–OH into a polyurethane system gives rise to the formation of binary polyurethane soft segments, which in turn leads to an enhancement in the cross-linking density of the system. This is accompanied by the formation of intermolecular hydrogen bonds that impede the relative sliding of the molecules, thereby increasing the tensile strength.[36] However, the tensile strength decreased with the addition of OH–PDMS–OH, probably because too much molecular weight of OH–PDMS–OH affected the density of effective crosslinking points in the PU, resulting in a decrease in the overall structural strength of the material. The tensile strength of the coating film decreased with the addition of superhydrophobically modified silica, which was attributed to the uneven dispersion of modified silica particles in the composite coating film to form aggregates, and these microscopic defects were highly susceptible to crack initiation and propagation when the material was subjected to stretching, ultimately leading to a decrease in mechanical properties.[37]

In a region from 300 to 800 nm in LAMBDA, the wavelength indicating transparency of the coating film is 500 nm. Fig. 3d shows that the polyurethane-coated film with no modifier added and the polyurethane-coated film with only OH–PDMS–OH added are transparent. The transparency of the coated film is observed to decrease with the addition of OH–PDMS–OH, yet it remains transparent. However, the incorporation of superhydrophobically modified $SiO_2$ results in the film becoming opaque.

### 3.3 Superhydrophobic surface tests

The hydrophobicity and antifouling properties of the polyurethane were improved by the addition of OH–PDMS–OH, and finally the polyurethane was brought to a superhydrophobic level by the addition of superhydrophobically modified meteorological nano-silica. Based on the superhydrophobic polyurethane composite coating film, three kinds of lossy properties that are easily encountered in daily life were investigated. First, contact angle tests were conducted on polyurethane-coated films prepared using all experimental protocols. Fig. 4a shows that the contact angle of the polyurethane coating film synthesized from the original soybean oil-based polyol was 86°. This angle was observed to increase to 122.9° when OH–PDMS–OH was introduced to the synthesis. To minimize the impact of petroleum-based polymers on the biobased content of the coating film, an experimental group of 20% P/PU coating films was selected for further investigation. Upon the addition of superhydrophobically modified $SiO_2$ up to 20% wt., the interfacial contact angle of the coating film reached 154.8°, indicating a transition from hydrophobicity to superhydrophobicity. A video of the superhydrophobic coating can be seen in Video S1.†

The coating film is capable of maintaining its physical and chemical properties in an acidic or alkaline environment, preventing degradation and ensuring its long-term hydrophobic properties. However, if these properties are not maintained, the coating film's applications in acidic or alkaline environments are significantly limited. Fig. 4b illustrates the deionized water control group. Solutions with varying pH values were prepared, and the samples were fully submerged in them. After 2 weeks, the samples were removed for contact angle testing. The results demonstrate that following immersion in disparate pH solutions, the contact angle of the coating film diminished, yet it retained its super-hydrophobicity at WCA = 150.1°. This evidence substantiates the assertion that the synthesized polyurethane coating film is well-suited for application in daily life environments.

The ability of superhydrophobic coatings to withstand abrasion is a critical factor that contributes to their extensive range of applications. A coating film that is both abrasion-resistant and stable is less susceptible to damage from external environmental factors and is capable of maintaining stable hydrophobicity over an extended period, thereby extending the service life of the coating. Fig. 4c shows the testing methodology employed for the superhydrophobic sample, which was placed face down on 2000 SiC sandpaper with a load weight of 100 g. The sample was then pulled horizontally by 10 cm at a constant speed, and the contact angles were measured after 500, 1000, 1500, and 2000 cycles, respectively. Following 2000 cycles of friction, the contact angle of the coating film exhibited a slight decrease. However, it remained superhydrophobic at WCA = 150.3°, indicating that the coating film has the potential to be utilized in abrasive environments. As illustrated in Fig. S1,† the maximum contact angle in this work is better than that of most of the fluorine-free superhydrophobic polyurethanes reported in the existing literature, and the superhydrophobic retention after sandpaper friction cycle testing is better than that of most existing superhydrophobic polyurethanes in the literature.[38–45]

As a protective coating film that can be applied outdoors, it is necessary to evaluate its performance under the influence of various environmental factors, including ultraviolet radiation, humidity, precipitation, and dust contamination. Fig. 4c shows the testing of superhydrophobic samples which were placed outside on the roof of an outdoor building for different periods and then retrieved and tested for the contact angle. The contact angle of the coating film exhibited a slight decrease. However, it remained superhydrophobic at WCA = 153.3°, indicating that the coating film has potential for use in outdoor protective coatings.

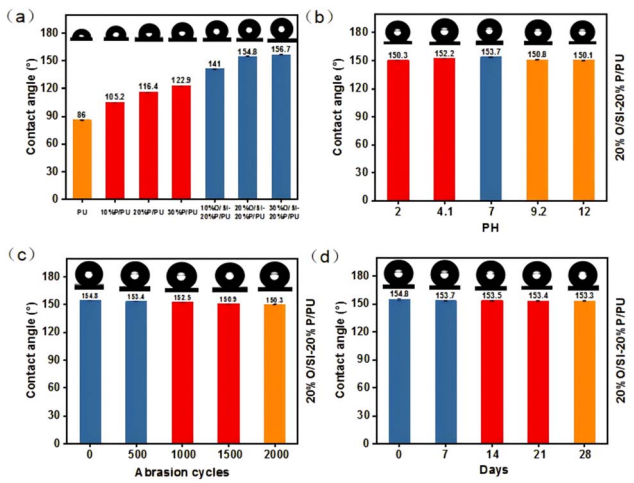


Fig. 4 The contact angle test graphs of the different experimental groups (a). The contact angle graphs after two weeks of immersion in various acid and alkali solutions (b). The contact angle graphs after different friction cycles (c). The contact angle graphs after different days of outdoor exposure (d).

### 3.4 Morphological studies of the hydrophobic coating film

Scanning electron microscopy enables the observation of thin coating film surfaces, providing information on surface roughness, texture, and pore structure. Fig. 5a displays the surface morphology of the unmodified polyurethane coating film, revealing its smooth texture and low adhesion to water droplets, which indicates its relatively good hydrophobicity.

Following the addition of OH–PDMS–OH, the microscopic morphology of the PU coating film exhibited a wrinkle-shaped alteration. This can be discerned through the surface elemental analysis depicted in EDS in Fig. 5b. The wrinkled region is characterized by an enrichment of silicon and oxygen elements, thereby indicating that the silicone cover layer is capable of forming a microscopic concave-convex structure on the surface of the coating film, which serves to increase the surface roughness and consequently enhances the contact angle between the coating film and the liquid, thereby resulting in a more hydrophobic surface. When superhydrophobically modified silica is added, it creates numerous tiny particles that adhere to the surface of the coated film. This is in addition to

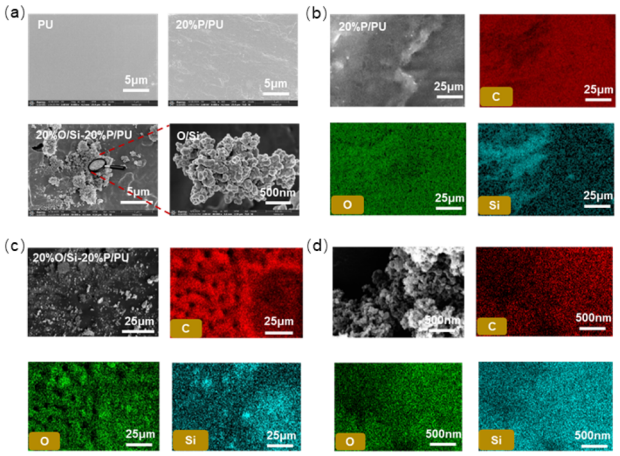


Fig. 5 The SEM testing of PU, 20% P/PU, 20% O/Si–20% P/PU, O/Si (a), the EDS results of 20% P/PU (b), the EDS results of 20% O/Si–20% P/PU (c), and the EDS results of O/Si (d).

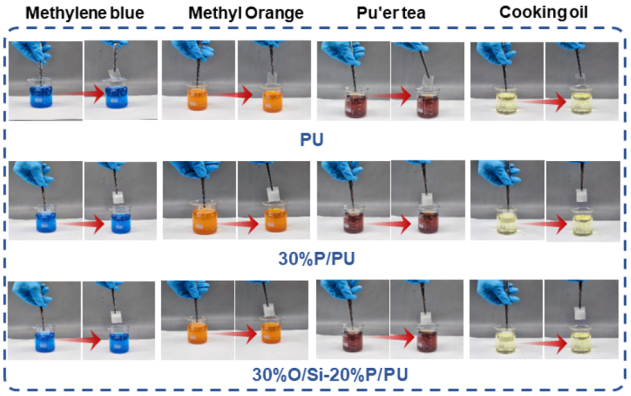


Fig. 6 The diagram of the antifouling application test process.

the fold-shaped bumps created by OH–PDMS–OH, which significantly enhances the surface roughness of the coated film, making it superhydrophobic.

Fig. 5c shows the modified silica addition to the PU coating film; the surface of the PU coating film showed a rough microscopic nanoscale structure. This is because the modified silica can increase the roughness and surface area of the surface, and this structure allows the water droplets to form a larger contact angle on the surface of the coating film, making it easier for the water droplets to slide on the surface and exhibit super-hydrophobicity. According to the micro-zone compositional analysis of the EDS in Fig. 5d, it is evident that the agglomerated round spheres, sized at 10 nm, are rich in silicon, oxygen, and carbon elements. This analysis confirms that these microspheres are hydrophobically modified silica.

The SEM and EDS analyses show that as the amount of OH–PDMS–OH and hydrophobically modified silica added increases, the microscopic surface of the membrane becomes progressively rougher. This change can account for the increase in the contact angle of the PU membrane from 86° to 156.7°. The detailed results of the SEM-EDS tests for all experimental groups are shown in Fig. S2 and S3.†

### 3.5 Antifouling application test

The ultimate goal of the superhydrophobic antifouling coating film is to achieve excellent liquid repellency and easy-to-clean self-cleaning properties. Fig. 6 shows that the objective of superhydrophobic antifouling coating films is to attain optimal liquid-repellent properties and straightforward self-cleaning capabilities. Polyurethane samples were vertically immersed in a series of common liquids, including methylene blue solution, methyl orange solution, pu-erh tea, and cooking oil, to study the coating films' antifouling ability. Upon removal of the coated films from water-soluble pollutants, it was observed that no liquid adherence occurred on the surface of all coated films, thereby demonstrating that the coated films possess excellent anti-fouling capabilities against water-soluble pollutants. However, in the pure polyurethane and the experimental group with the addition of OH–PDMS–OH, it can be observed that there are notable residual deposits of oily pollutants on the surface of the coating film. Following the addition of super-hydrophobically modified $SiO_2$, it was observed that oily pollutants gradually converged to the bottom and could be easily wiped away with a paper towel. This demonstrates that the coating film exhibits dual characteristics of super-hydrophobicity and oil repellency after adding super-hydrophobically modified $SiO_2$. The results of the antifouling tests for all experimental groups are presented in detail in Fig. S4.†

## 4. Conclusion

Bio-based polyols with highly reactive groups, containing a hydroxyl value of 1.89 mm $g^{-1}$, were synthesized from epoxidized soybean oil and mono-ethyl itaconic acid as raw materials with monothioglycerol in a two-step process. The synthesized polyurethane is transparent and has good flexibility in 18 MPa and WCA = 80°. Polyurethanes with binary soft segments were prepared using OH–PDMS–OH as an antifouling agent. Subsequently, during the synthesis of the polyurethane, a super-hydrophobic antifouling coating film was obtained by blending superhydrophobically modified nano-$SiO_2$ to form a rough microstructure inside and on the surface of the coating film and $WCA_{max}$ = 156.7°. The coating film retained its super-hydrophobic and oil- and dirt-resistant properties after 2000 friction cycles, immersion in acid and alkali solutions, and outdoor placement for 28 days. The bio-based polyurethane coating film exhibited long-lasting super-hydrophobicity and oil- and dirt-resistant properties, which provide a promising solution for future indoor and outdoor antifouling protective coating films.

## Data availability

The data that support the findings of this study are available on request from the corresponding author. The data are not publicly available due to privacy or ethical restrictions.

## Author contributions

Junming Huang: writing – review & editing. Genzheng Sha: formal analysis, writing – review & editing. Minghui Cui: formal analysis, writing – review & editing. Mengqiu Quan: writing – review & editing. Yuqing Wang: formal analysis, writing – review & editing. Yao Lu: project administration, writing – review & editing. Jin Zhu: project administration, writing – review & editing. Jing Chen: supervision, project administration, writing – review & editing.

## Conflicts of interest

The authors declare that they have no known competing financial interests or personal relationships that could have appeared to influence the work reported in this paper.

## Acknowledgements

This work was financially supported by the National Key Research and Development Program of China (2017YFE0102300), the S&T Innovation 2025 Major Special Program of Ningbo (2022Z139), the National Natural Science Foundation of China (U21B2093 and U23A20691) and the Scientific Research Funding Project of the Educational Department of Liaoning Province in 2024 (LJ212410149017).

## References

1 Y. Li, Y. Jin, R. Zhou, W. Zeng and J. Mei, *Prog. Org. Coat.*, 2024, **190**, 108386.
2 S. Duan, J. Cui, J. Hu, T. Han, Y. Chen, H. Wang and T. Ma, *Constr. Build. Mater.*, 2024, **438**, 137236.
3 G. Zhu, M. Wu, Z. Ding, T. Zou and L. Wang, *Eur. Polym. J.*, 2023, **201**, 112536.
4 X. Su, W. Yang, Z. Zhang, L. Deng, K. Li, H. Xie, Y. Wu, X. Zhang and W. Wu, *ACS Appl. Nano Mater.*, 2024, **7**, 2164–2175.
5 Y. Su, Y. Xu, H. Wang, S. Dong, X. Cheng and H. Wang, *Prog. Org. Coat.*, 2024, **195**, 108639.
6 A. Kemona and M. Piotrowska, *Polymers*, 2020, **12**, 1752.
7 A. Delavarde, G. Savin, P. Derkenne, M. Boursier, R. Morales-Cerrada, B. Nottelet, J. Pinaud and S. Caillol, *Prog. Polym. Sci.*, 2024, **151**, 101805.
8 H. Lu, C. Dun, H. Jariwala, R. Wang, P. Cui, H. Zhang, Q. Dai, S. Yang and H. Zhang, *J. Controlled Release*, 2022, **350**, 748–760.
9 J. Li, C. Hong, J. Zhang, R. Zhai, Y. Han, M. Liu, Y. Wang, Y. Song and C. Zhou, *Prog. Org. Coat.*, 2024, **189**, 108340.
10 M. H. Tran and E. Y. Lee, *Environ. Chem. Lett.*, 2023, **21**, 2199–2223.
11 H. Q. Chu, X. Y. Yu, H. T. Jiang, D. D. Wang and N. Xu, *Int. J. Heat Mass Transfer*, 2023, **200**, 26.
12 H. Attia, D. J. Johnson, C. J. Wright and N. Hilal, *Desalination*, 2018, **446**, 70–82.
13 Y. Yang, Z. Guo and W. Liu, *J. Hazard. Mater.*, 2024, **461**, 132592.
14 H. Li, L. Xin, J. Gao, Y. Shao, Z. Zhang and L. Ren, *Small*, 2024, **20**, 2309012.
15 Y. Shen, Z. Wu, J. Tao, Z. Jia, H. Chen, S. Liu, J. Jiang and Z. Wang, *ACS Appl. Mater. Interfaces*, 2020, **12**, 25484–25493.
16 H. Wang, H. Hu, C. Zhou, W. Wei, B. Fan, H. Wang and S. Dong, *Prog. Org. Coat.*, 2023, **183**, 107799.
17 Y. Zhang, D. Wang, Z. Huang, H. Zhang and L. Li, *J. Membr. Sci.*, 2022, **662**, 121000.
18 H.-M. Kim, J. Lee, J. Seo and J.-H. Seo, *Colloids Surf., A*, 2019, **572**, 47–57.
19 Y. H. Lei, B. C. Jiang, H. Liu, F. Zhang, Y. An, Y. L. Zhang, Y. Yuan, J. X. Xu, X. F. Li and T. Liu, *Prog. Org. Coat.*, 2023, **183**, 107795.
20 H. Zheng, Z. Lai and G. Liu, *Adv. Funct. Mater.*, 2023, **34**, 2312543.
21 P. K. Behera, P. Mondal and N. K. Singha, *Macromolecules*, 2018, **51**, 4749–4986.
22 X. Zhang, D. Lin, Z. Liu, S. Yuan, X. Wang, H. Wang and J. Wang, *J. Alloys Compd.*, 2021, **886**, 161156.
23 B. Q. H. Nguyen, A. Shanmugasundaram, T.-F. Hou, J. Park and D.-W. Lee, *Chem. Eng. J.*, 2019, **373**, 68–77.
24 S. Roshan, A. A. Sarabi, R. Jafari and G. Momen, *Prog. Org. Coat.*, 2022, **169**, 106918.
25 L. N. Lv, H. Liu, W. Zhang, J. Y. Chen and Z. Z. Liu, *Mater. Lett.*, 2020, **258**, 126653.
26 Q. Li, L. Guo, T. Qiu, W. Xiao, D. Du and X. Li, *Appl. Surf. Sci.*, 2016, **377**, 66–74.
27 S. Xu, L. Xie, X. Yu, Y. Xiong and H. Tang, *J. Polym. Sci., Part A: Polym. Chem.*, 2015, **53**, 1794–1805.
28 A. Khan, K. Huang, M. G. Sarwar, K. Cheng, Z. Li, M. O. Tuhin and M. Rabnawaz, *J. Colloid Interface Sci.*, 2020, **577**, 311–318.
29 X. Wang, Z. B. Wang, L. P. Heng and L. Jiang, *Adv. Funct. Mater.*, 2020, **30**, 1902686.
30 F. Khan, M. Rabnawaz, Z. Li, A. Khan, M. Naveed, M. O. Tuhin and F. Rahimb, *ACS Appl. Polym. Mater.*, 2019, **1**, 2659–2667.
31 S. S. Xia, Y. Pang, Z. X. Yu, J. Wang and Z. Q. Chen, *J. Environ. Chem. Eng.*, 2023, **11**, 110605.
32 P. Li, S. Ma, J. Dai, X. Liu, Y. Jiang, S. Wang, J. Wei, J. Chen and J. Zhu, *ACS Sustain. Chem. Eng.*, 2017, **5**, 1228–1236.
33 Q. Yu, Z. Zhang, P. Tan, J. Zhou, X. Ma, Y. Shao, S. Wei and Z. Gao, *Polymers*, 2023, **15**, 4588.
34 P. Li, S. Ma, J. Dai, X. Liu, Y. Jiang, S. Wang, J. Wei, J. Chen and J. Zhu, *ACS Sustain. Chem. Eng.*, 2016, **5**, 1228–1236.
35 Z. Cheng, Q. Li, Z. Yan, G. Liao, B. Zhang, Y. Yu, C. Yi and Z. Xu, *Prog. Org. Coat.*, 2019, **127**, 194–201.
36 L. Meng, H. Qiu, D. Wang, B. Feng, M. Di, J. Shi and S. Wei, *Prog. Org. Coat.*, 2020, **140**, 105492.
37 R. C. R. Nunes, J. L. C. Fonseca and M. R. Pereira, *Polym. Test.*, 2000, **19**, 93–103.
38 S. Huang, G. Liu, K. Zhang, H. Hu, J. Wang, L. Miao and T. Tabrizizadeh, *Chem. Eng. J.*, 2019, **360**, 445–451.
39 X. Zhan, J. Chen, Z. Yang, G. Wu and Z. Kong, *Int. J. Biol. Macromol.*, 2023, **232**, 123431.
40 H. Wang, L. Chen, Y. Yi, Y. Fu, J. Xiong and N. Li, *ACS Appl. Nano Mater.*, 2022, **5**, 10686–10695.

41 M. Liu, Y. Luo and D. Jia, *Compos. Sci. Technol.*, 2020, **197**, 108231.
42 Y. Lei, B. Jiang, H. Liu, F. Zhang, Y. An, Y. Zhang, Y. Yuan, J. Xu, X. Li and T. Liu, *Prog. Org. Coat.*, 2023, **183**, 107795.
43 X. Chen, Z. Yin, Y. Deng, Z. Li, M. Xue, Y. Chen, Y. Xie, W. Liu, P. He, Y. Luo, Z. Hong and C. Xie, *Sens. Actuators, A*, 2023, **362**, 114630.
44 L. Lv, H. Liu, W. Zhang, J. Chen and Z. Liu, *Mater. Lett.*, 2020, **258**, 126653.
45 P. Fu, J. Ou, Y. He, Y. Hu, F. Wang, X. Fang, W. Li and A. Amirfazli, *Surf. Interfaces*, 2024, **45**, 103890.